JOURNAL OF Applied Polymer SCIENCE

Preparation and Characterization of 2-Methacryloyloxyethyl Phosphorylcholine Polymer Nanofibers Prepared via Electrospinning for Biomedical Materials

Tomoki Maeda,[1]* Katsuya Hagiwara,[1]* Soki Yoshida,[1] Terumitsu Hasebe,[1,2] Atsushi Hotta[1]

[1]Department of Mechanical Engineering, Keio University, Yokohama 223-8522, Japan

[2]Tokai University Hachioji Hospital, Tokai University School of Medicine, Tokyo 190-0032, Japan

*These authors contributed equally to this work.

Correspondence to: A. Hotta (E-mail: hotta@mech.keio.ac.jp)

ABSTRACT: Electrospun nanofibers of poly (2-methacryloyloxyethyl phosphorylcholine) (MPC) possessing excellent hemocompatibility were successfully fabricated first. These nanofibers were investigated as drug-delivery vehicles for suppressing the acute thrombogenicity of vascular grafts to lower the risk of coronary artery disease by improving the graft patency rate; the graft patency rate is the percentage of patients who do not have any blockage in a graft after a stent-graft treatment. We varied the MPC concentrations in ethanol from 1 to 10 wt % to fabricate electrospun MPC fibers. Scanning electron microscopy images revealed that when the MPC concentration was lower than 5 wt %, beads instead of fibers were formed. When the MPC concentration was increased (>5 wt %), uniform fibers were produced with average fiber diameters of about 160 nm (5 wt %), 640 nm (7.5 wt %), and 1270 nm (10 wt %). *In vitro* drug-release tests showed that a higher amount of drugs was diffused from MPC fibers with small diameters; this indicated a faster drug-release rate for the thinner MPC fibers. Diameter-controlled MPC fibers could be used as a new vascular graft materials.
 J. Appl. Polym. Sci. **2014**, *131*, 40606.

KEYWORDS: biomaterials; drug-delivery systems; electrospinning; fibers; phospholipids

Received 30 December 2013; accepted 23 February 2014

DOI: 10.1002/app.40606

INTRODUCTION

Cardiovascular diseases have become increasingly common among elderly adults, and about 4.3 million people per year in Europe die of cardiovascular disease.[1] The blockage of blood flow by, for example, arteriosclerosis could cause a significant clinical burden. If arteriosclerosis can be detected early, many blockage areas can be bypassed or replaced by vascular substitutes, including arterial autografts made of polytetrafluoroethylene (PTFE) and polyester. However, the graft patency rate (the percentage of patients who do not have any blockage in the graft after a stent-graft treatment) after 24 months of such arterial autografts is still not high enough; it is only 47% for PTFE and 54% for polyester grafts.[2] It was reported that one of the major reasons for the low patency rate is the acute thrombogenicity of the grafts.[3–5]

Several studies have been attempted with limited success to reduce the thrombogenicity of the grafts to improve the patency rate. Among them, the addition of antithrombotic factors to reduce thrombogenicity or coating with the cell growth factor to promote endothelialization has been the most frequently studied graft modification. However, there has been a growing concern that most drugs are swiftly released from the graft surface in the early stages of drug release. Thus, controlled drug release from the polymers is highly demanded for vascular grafts. As for the coating, the cell growth factors could indeed provide excellent antithrombogenic properties, but the growth factors could also support platelet and smooth muscle cell adhesion and proliferation, which could possibly lead to serious thrombosis.

Electrospun fibers have been widely studied as materials for vascular grafts; they present satisfactory biomedical performances, such as antithrombogenicity, cell compatibility, and patency rates equal to or even superior to current standard PTFE grafts.[6–8] Electrospinning is a simple method for producing fibrous materials with diameters ranging from nanometers to micrometers. The electrospun fibers could establish three-dimensional scaffolds possessing a high surface area and high porosity with effective pore size control; they could find practical applications in areas such as tissue engineering scaffolds. The architectural properties of scaffolds, such as fiber diameters and porosity, depend on the physical electrospinning parameters

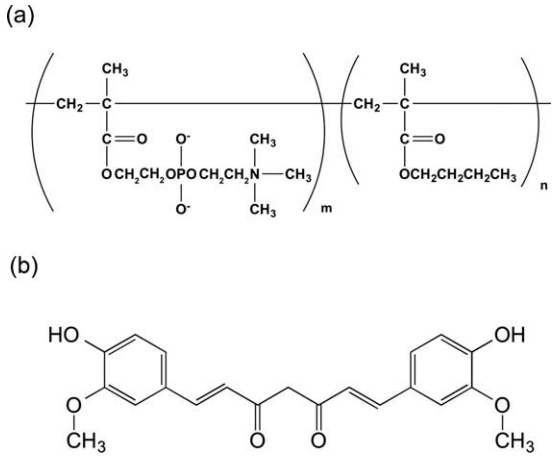

Figure 1. Chemical structures of (a) MPC and (b) curcumin; *m* and *n* represent the degree of polymerization of each polymeric segment.

such as the solution viscosity, surface tension, conductivity, and processing conditions. The scaffold properties eventually and significantly affect the biological reaction between the material surface and the cells. It was found that the scaffold porosity enhanced the cell infiltration *in vitro*[9,10] and the tissue integration *in vivo*.[11] It was also reported that endothelialization was improved on scaffolds with nanofibers as compared with those with microfibers.[12,13] Electrospinning has also been recently explored as a new device producing fibers for drug delivery.[14–16] Drug-release profile could be well controlled by the scaffold properties such as fiber diameters and porosity that could be changed by the electrospinning parameters.[17]

In this work, we focused on the electrospinning of poly (2-methacryloyloxyethyl phosphorylcholine) (MPC), one of the most frequently studied phospholipid polymers that exhibit excellent hemocompatibility.[18,19] The fabrication of MPC fibers by electrospinning process has not been reported yet, and in this research, the fabrication procedures of MPC fibers were thoroughly investigated, and the drug-delivery characteristics from the electrospun MPC fibers were examined. The possibility of controlling the drug-release rate by varying the diameter of MPC fibers was also explored. The rather preliminary experimental results of our works have proved that the MPC nanofibers could be a promising candidate for cardiovascular graft materials with effective and controlled drug release.

EXPERIMENTAL

Materials

MPC was selected as typical biocompatible polymers. It is well known that the surface of the MPC polymers mildly interacts with blood components. The chemical structure of MPC was presented in Figure 1(a). MPC with the molecular weight of 500,000 was supplied by Terumo Clinical Supply Co., Ltd. The block ratio of each chemical block (*m*:*n*) in MPC was 3:7. Curcumin, an antithrombogenic, antioxidant, and antiproliferating agent, was selected as an eluting drug. Curcumin is a major chemical component of turmeric, which inhibits platelet-derived growth factor/stimulated vascular smooth muscle cell migration, proliferation, and collagen synthesis, which are all key events related to cardiovascular disease.[20] The chemical structure of curcumin is displayed in Figure 1(b). Curcumin, with a molecular weight of 368.38, was purchased from Sigma-Aldrich Co., Ltd.

Preparation of the MPC Solution and Electrospinning Process

The 1, 2, 3, 4, 5, 7.5, and 10 wt % solutions of MPC were prepared in ethanol at room temperature. Then, curcumin was added to the solution, as illustrated in Table I. We fixed the mass ratio of curcumin to MPC. The mixture was stirred for 24 h at room temperature to ensure a complete dissolution of curcumin when a homogeneous composite solution was eventually obtained for electrospinning. The MPC fibers were electrospun onto an aluminum plate. The electrospinning setup consisted of a syringe, a needle, and a high-voltage power supply (HER-30P1, Matsusada Precision Co., Ltd.). A high voltage of 12.5 kV was applied between the syringe needle (i.e., the polymer solution) and the earth. A voltage of 12.5 kV was the minimum needed to fabricate fibers stably. The aluminum plate was separated 10 cm horizontally from the needle. As in our experimental conditions, we placed the syringe parallel to the ground, and the height from the ground to the needle tip was less than 12 cm. It was necessary to place the aluminum plate at the point less than 12 cm to neglect the effect of the ground. The MPC solution was extruded from the syringe at a rate of 0.5 mL/h, the well-used flow rate, which was known to have not influenced the diameter of fibers. The electrospun MPC fibers were dried in a vacuum oven (VOS-201SD, EYELA Co., Ltd.) at room temperature for 24 h to remove the residual solvent. A simple solvent-cast MPC film with curcumin was also made as a reference for comparison: MPC was dissolved in ethanol at 5 wt % before curcumin was added to the MPC solution at 4 wt % against the MPC mass. The MPC solution was cast onto an aluminum plate, which was slowly dried in air to evaporate the solvent, and the substrates were kept *in vacuo* for more than 24 h to completely eliminate any residual solvent. We named the samples as the *film* for the MPC film with curcumin prepared by solvent casting, *160 nm* for the MPC fibers of 164 nm with curcumin, *640 nm* for the MPC fibers of 637 nm with curcumin, and finally, *1270 nm* for the MPC fibers of 1270 nm with curcumin.

Fiber Morphologies

The surface morphologies of the fiber structure were observed by scanning electron microscopy (SEM; S-2380N, Hitachi Co., Ltd.) and atomic force microscopy (AFM; SPM9700, SHIMADZU Co., Ltd.). SEM was carried out at an accelerating voltage of 5 kV. Before SEM observation, according to the general procedure of preventing electrostatic charges against the

Table I. Solution Composition Ratios of Each MPC Sample

Sample	Ethanol	MPC	Curcumin
Film	95.0	5.0	0.2
MPC fiber 5.0 wt %	95.0	5.0	0.2
MPC fiber 7.5 wt %	92.5	7.5	0.3
MPC fiber 10 wt %	90.0	10	0.4

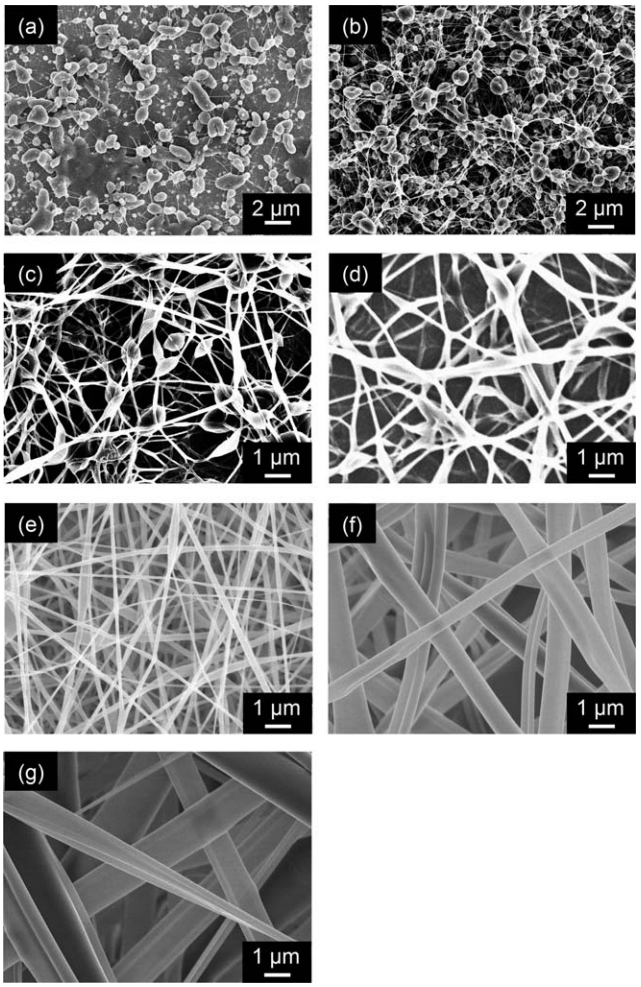

Figure 2. SEM images of the electrospun MPC fibers: (a) 1, (b) 2, (c) 3, (d) 4, (e) 5, (f) 7.5, and (g) 10 wt %.

polymers, all of the MPC fiber specimens that were formed into a sheet (2×2 cm^2) were coated with osmium for 15 s with an ion osmium coater (HPC-1 SW, Vacuum Device, Inc.), where the applied voltage was 700 V and the current was 3–5 mA. The total pressure was kept at 13 Pa. The thickness of osmium was approximately 5 nm. The fiber diameters of each sample were calculated by the free image processing software called Image J (ver. 1.47). The surface roughness (R_a) of each sample was investigated by AFM. The surface area was calculated mathematically from the configuration of the samples. For the film, we directly calculated the area of the film surface contacting the medium. For the fibers, we calculated the area of the fibers from the diameter of the fibers.

Water Contact Angle Measurements

The wettability of each MPC specimen was evaluated by the measurement of the static contact angles of droplets of distilled water (5.0 μL each) on the sample surfaces. The contact angle measurements were conducted with the sessile drop method with a contact angle meter (DM500, Kyowa Interface Science Co., Ltd.). After the specimens were stabilized in air for 1 day, the contact angle measurements were carried out at five different locations of each specimen at room temperature. The results of the measurements are expressed as the mean of five replicates along with the standard deviation.

Fourier Transform Infrared (FTIR) Spectral Analysis

The chemical structures of the MPC fibers containing curcumin were examined by attenuated total reflectance–FTIR spectroscopy (ALPHA-E, Bruker Co., Ltd.). ZnSe was used for the attenuated total reflectance crystal. The scanning wave numbers ranged from 4000 to 400 cm^{-1}. The spectrum resolution was 2 cm^{-1}, and the 200 scans were accumulated to determine one spectrum. For FTIR analysis, we used solid MPC nanofibers containing 4 wt % curcumin with a diameter of 160 nm from the 5 wt % MPC solution. We also prepared original MPC fibers without curcumin as a control.

In Vitro Drug-Release Tests

Each MPC specimen was soaked in 2 mL of medium with phosphate-buffered saline at pH 7.4 and 37°C. The medium was removed and collected every 24 h to measure the concentration of the curcumin in medium extracted from the MPC specimens. After the medium was removed for the concentration experiments, it was replaced with new fresh medium to examine the next stage of curcumin elution. The *drug-release/elution time* was defined as the immersion time of the samples in phosphate-buffered saline. The elution time at 0 days was the time when we started the drug-release testing. The concentration of the extracted curcumin in the medium was measured by ultraviolet–visible spectroscopy (U-2810, Hitachi, Co., Ltd.). The wavelength for ultraviolet–visible testing ranged from 400 to 500 nm. The concentration of curcumin was calculated with the Lambert–Beer equation ($A = \varepsilon cl$, where A is the absorbance, ε is the molar absorbance coefficient, c is the concentration, and l is the length of the light path) and eventually converted to the weight of the eluted curcumin by analysis of the UV absorbance of raw curcumin dissolved in fresh medium. In our experiments, ε was 49.1×10^4 (L/mol cm), and l was 1 cm. The results were plotted as cumulative micrograms of the eluted drug as a function of the drug releasing/elution time.

Characterization of the MPC-Covered Stent

Balloon-expandable metallic stents made of cobalt–chromium alloy (12 mm in length, 3 mm in outer diameter, and 0.06 mm in thickness; Japan Stent Technology Co., Ltd., Japan) were used for the test production. Here, the MPC nanofibers were electrospun onto the metallic stents, which were rotated at about 60 rpm. The fabrication of the MPC nanofibers was carried out for approximately 1 h under the same conditions described in the previous section. The MPC-covered stent was observed by SEM after 24 h in a vacuum.

RESULTS AND DISCUSSION

Surface Morphology of the MPC Fibers

The diameters and morphologies of the electrospun fibers were mainly influenced by two factors: the electrospinning process parameters (e.g., applied voltage, collection distance) and the solution properties (e.g., surface tension, viscosity, conductivity), which were strongly dependent on the polymer concentration. In this study, we only varied the MPC concentrations from 1 to 10 wt % to change the solution properties, especially the viscosity of

Table II. Fiber Diameters and R_a Values of Each MPC Sample as Determined by AFM and Image J Software

Weight percentage in ethanol	Fiber diameter (nm)	R_a (nm)
5.0	163.5 ± 73.2	273 ± 6
7.5	636.5 ± 198	276 ± 6
10	1265 ± 451	388 ± 10

the solution, whereas the electrospinning process parameters were fixed. Thus, the diameter and the morphology of fibers were determined by the MPC concentrations in the experiments.

The SEM images of each MPC fiber containing curcumin are presented in Figure 2. When we analyzed the SEM images, we found that when the MPC concentration was lower than 5 wt %, beads were formed. With increasing MPC concentration, fibers were obtained instead of beads, and they became dominant. Different MPC fiber diameters could be obtained by different MPC concentrations: the average synthesized fiber diameters were approximately 160 nm for the 5 wt % MPC solution, 640 nm for the 7.5 wt % MPC solution, and 1270 nm for 10 wt % MPC solution, as listed in Table II. As was already mentioned in the Experimental section, *film* refers to the MPC film, *160 nm* refers to the MPC fibers of 164 nm, *640 nm* refers to the MPC fibers of 637 nm, and *1270 nm* refers to the MPC fibers of 1270 nm, all specimens with curcumin. It is well known that the higher solution viscosity obtained when the polymer concentration increased resulted in an increase in the fiber diameter.[21]

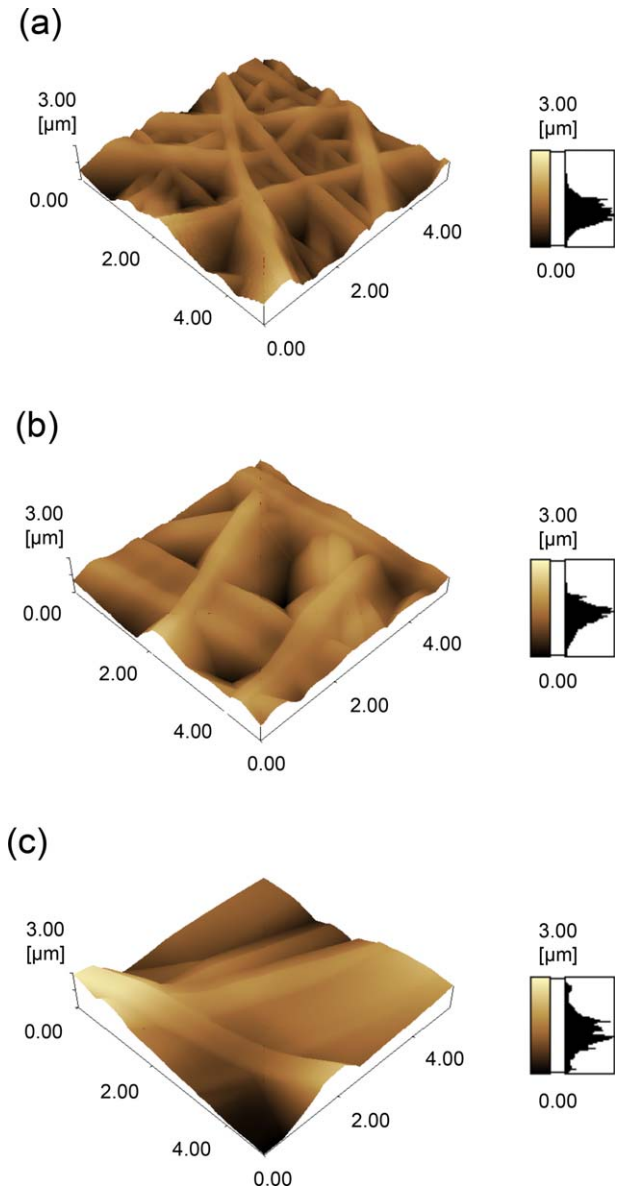

Figure 3. AFM images of the electrospun MPC fibers: (a) 5, (b) 7.5, and (c) 10 wt %. [Color figure can be viewed in the online issue, which is available at wileyonlinelibrary.com.]

The AFM results of each fiber are shown in Figure 3. The MPC fibers, especially 160 and 640 nm, presented typical structures of three-dimensional scaffolds. Such structures could provide a relatively high surface area considering the original volume. The 1270 nm MPC fibers made from the 10 wt % MPC solution were not clearly observed by AFM because of their high R_a. The R_a of each sample is shown in Table II. The SEM and AFM images indicate that we successfully fabricated MPC nanofibers and microfibers possessing three-dimensional structures when the MPC concentrations were 5.0, 7.5, and 10 wt %. We also found that the diameters of the MPC fibers were well controlled through the variation of the MPC concentrations.

Water Contact Angle Measurements of the MPC Fibers

Figure 4 shows the results of the contact angles of the distilled water droplets on each surface of the MPC film and the MPC fibers. The water contact angle of the MPC film was rather high at about 100° because of the hydrophobic molecular block in the MPC polymer. The electrospun MPC fibers possessed higher contact angles than the MPC film. Moreover, with increasing MPC concentration and, thus, with increasing MPC fiber diameter, the contact angle increased. Such increase in the contact angles observed for the MPC fibers could have been due to the increase in R_a.

Chemical Structures of the MPC Fibers Containing Curcumin

Figure 5 shows the FTIR spectra of the MPC fibers: the original solid MPC fibers with the diameter of 160 nm without

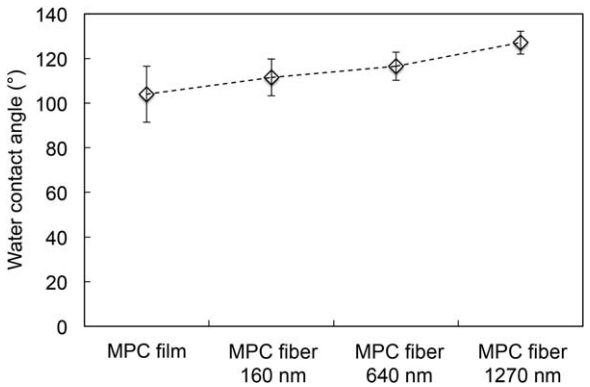

Figure 4. Contact angles of the distilled water droplets on each MPC sample.

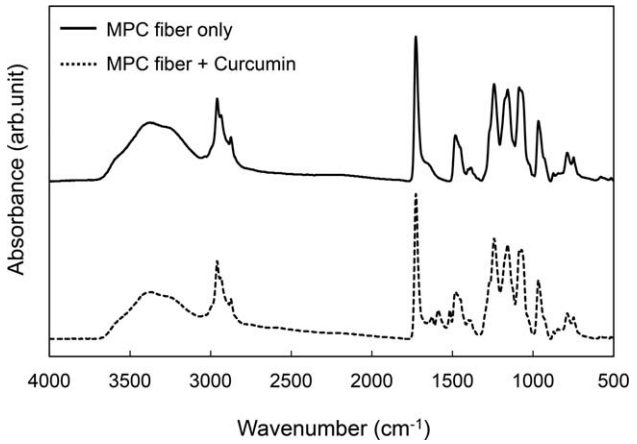

Figure 5. FTIR spectra of the MPC fibers and MPC fibers with curcumin.

curcumin and the solid MPC fibers with the diameter of 160 nm containing 4 wt % curcumin. We carefully analyzed the spectrum of the MPC fibers containing 4 wt % curcumin to detect the curcumin signal considering the MPC signal emitted by the original MPC fibers. During the analysis of the FTIR spectra, it was important to determine the difference between the molecular structures of the MPC fibers.

The spectrum of MPC fibers is presented in Figure 5. The broad signal detected around 3400 cm^{-1} was attributed to —OH vibrations from hydrogen-bonded —OH groups. Both MPC and curcumin possess hydrogen-bonded —OH groups in their molecular structures. The strong peaks at 2959, 2866, and 1474 cm^{-1} were attributed to the stretching of $—CH_2—$ groups. One of the major characteristic peaks of MPC is a stretching vibration peak observed at 1724 cm^{-1} by —(C=O)—O— of ester. The three peaks at 1234, 1152, and 1076 cm^{-1} were due to $—POCH_2—$.

As for the IR signal of the curcumin, the peak at 1620 cm^{-1}, which indicated the existence of aromatic —C=C—, was found in the spectrum of each MPC fiber containing curcumin. We found that the MPC fibers containing curcumin were successfully fabricated even when the diameter of MPC fibers was reduced.

Release Profile of Curcumin from the MPC Fibers

The cumulative released amount of curcumin from the MPC film and the MPC fibers to the medium as a function of time is plotted in Figure 6. All of specimens in Figure 6 contained 4 wt % curcumin. The circles, triangles, crosses, and squares in the graph represent the drug-release behaviors of film (MPC film) and 160, 640, and 1270 nm (the MPC fibers electrospun by 5, 7.5, and 10 wt % MPC solutions), respectively.

The MPC film presented a significant burst release in the early stage of the drug-release/elution time. Because MPC microfibers 1270 nm (with a diameter of 1270 nm) did not present such an initial burst release as was observed in the MPC film, the 1270 nm MPC microfiber showed only a slight improvement in the drug release, and the released amount was less than that of the film in the experimental time frame. The 160 and 640 nm MPC nanofibers (with diameters of 160 and 640 nm), on the other hand, possessed well-enhanced drug-release features without an

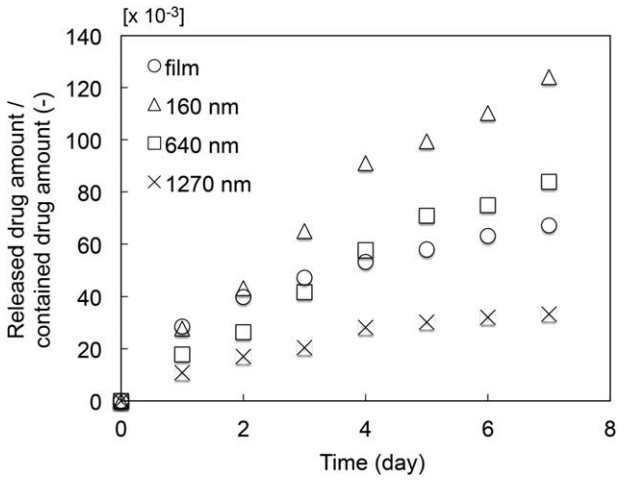

Figure 6. Drug-release profiles of the MPC film and MPC fibers with diameters of 164, 637, and 1270 nm.

initial burst release in the early stage of drug release, and hence, we concluded that the drug-release rate was well controlled by the decrease in the diameter of the MPC nanofibers. The released amount became larger with the decrease in the diameter of the fibers. This tendency could have been due to the increase in the specific surface area caused by the reduction of the fiber diameter, as shown in Figure 7. Higuchi reported the famous and probably the most often used mathematical equation describing the release rate of drugs from matrix systems. The basic equation of the Higuchi model is as follows:

$$M_t = A\sqrt{D(2c_0 - c_s)c_s t} \quad \text{for } c_0 > c_s$$

where M_t is the cumulative absolute amount of drug released at time t, A is the surface area of the controlled release device exposed to the release medium, D is the drug diffusivity in the polymer carrier, and c_0 and c_s are the initial drug concentration and the solubility of the drug in the polymer, respectively. In this study, when we changed the diameter of the MPC fibers, the surface area of the MPC fibers changed accordingly. As a result, we could control the drug-release rate from MPC by changing the surface area of the MPC fibers. The drug release and its rate were strongly related to the diameter of the nanofibers.

Characterization of the MPC-Covered Stent

The structures of the fibers on the metallic stents were observed by SEM. An SEM micrograph of the MPC-covered stent is

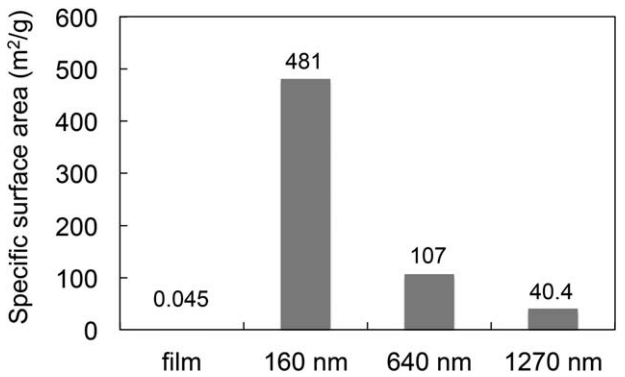

Figure 7. Specific surface area per unit mass of each sample.

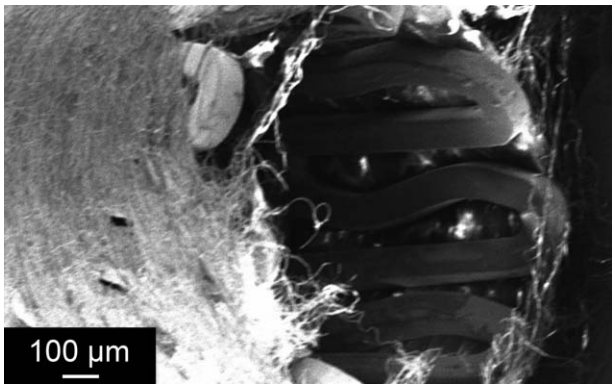

Figure 8. SEM image of the MPC-fiber-covered stent.

shown in Figure 8. The MPC fibers were efficiently synthesized, collected on the outer peripheral surface of the stent, and the fibers were almost aligned along the direction of the stent rotation during the electrospinning.

CONCLUSIONS

Diameter-controlled electrospun MPC nanofibers and microfibers were successfully produced by electrospinning, and their drug-release characteristics were investigated. The morphology of the MPC fibers fabricated by the electrospinning method was confirmed by SEM. We found that the increase in MPC content of the solution brought about an increase in the diameters of the MPC fibers. The drug-release rates from the electrospun MPC fibers were well controlled and enhanced by a decrease in the diameters of the MPC fibers. Our experimental results may be highly applicable to next-generation vascular grafts that possess both biocompatibility and well-controlled drug-release characteristics to prevent thrombosis.

ACKNOWLEDGMENTS

This work was supported in part by a Grant-in-Aid for Scientific Research (B; contract grant number 23360294, to A.H.), a Grant-in-Aid for Scientific Research (S; contract grant number 21226006, to A.H.), a Grant-in-Aid for Scientific Research for Challenging Exploratory Research (contract grant number 24656395, to A.H.) from the Japan Society for the Promotion of Science (JSPS KAKENHI), and by a Ministry of Education, Culture, Sports, Science and Technology (MEXT) Grant-in-Aid for the Program for Leading Graduate Schools (to T.M.).

REFERENCES

1. Stehouwer, C. D.; Clement, D.; Davidson, C.; Diehm, C.; Elte, J. W.; Lambert, M.; Sereni, D. *Eur. J. Intern. Med.* **2009**, *20*, 132.
2. Twine, C. P.; McLain, A. D. *Cochrane Database Syst. Rev.* **2010**, *5*, Cd001487.
3. Cho, S. W.; Lim, J. E.; Chu, H. S.; Hyun, H. J.; Choi, C. Y.; Hwang, K. C.; Yoo, K. J.; Kim, D. I.; Kim, B. S. *J. Biomed. Mater. Res. A* **2006**, *76*, 252.
4. Isenberg, B. C.; Williams, C.; Tranquillo, R. T. *Circul. Res.* **2006**, *98*, 25.
5. McClure, M. J.; Sell, S. A.; Simpson, D. G.; Walpoth, B. H.; Bowlin, G. L. *Acta Biomater.* **2010**, *6*, 2422.
6. Pektok, E.; Nottelet, B.; Tille, J. C.; Gurny, R.; Kalangos, A.; Moeller, M.; Walpoth, B. H. *Circulation* **2008**, *118*, 2563.
7. Oh, B.; Lee, C. H. *Mol. Pharm.* **2013**, *10*, 4432.
8. Kuraishi, K.; Iwata, H.; Nakano, S.; Kubota, S.; Tonami, H.; Toda, M.; Toma, N.; Matsushima, S.; Hamada, K.; Ogawa, S.; Taki, W. *J. Biomed. Mater. Res. B Appl. Biomater* **2009**, *88*, 230.
9. Baker, B. M.; Gee, A. O.; Metter, R. B.; Nathan, A. S.; Marklein, R. A.; Burdick, J. A.; Mauck, R. L. *Biomaterials* **2008**, *29*, 2348.
10. Milleret, V.; Simona, B.; Neuenschwander, P.; Hall, H. *Eur. Cell. Mater.* **2011**, *21*, 286.
11. Leong, M. F.; Chian, K. S.; Mhaisalkar, P. S.; Ong, W. F.; Ratner, B. D. *J. Biomed. Mater. Res. A* **2009**, *89*, 1040.
12. Ju, Y. M.; Choi, J. S.; Atala, A.; Yoo, J. J.; Lee, S. *J. Biomaterials* **2010**, *31*, 4313.
13. Kwon, I. K.; Kidoaki, S.; Matsuda, T. *Biomaterials* **2005**, *26*, 3929.
14. Xie, Z. W.; Buschle-Diller, G. *J. Appl. Polym. Sci.* **2010**, *115*, 1.
15. Wang, M.; Wang, L.; Huang, Y. *J. Appl. Polym. Sci.* **2007**, *106*, 2177.
16. Luong-Van, E.; Grondahl, L.; Chua, K. N.; Leong, K. W.; Nurcombe, V.; Cool, S. M. *Biomaterials* **2006**, *27*, 2042.
17. Moroni, L.; Licht, R.; de Boer, J.; de Wijn, J. R.; van Blitterswijk, C. A. *Biomaterials* **2006**, *27*, 4911.
18. Ishihara, K.; Ziats, N. P.; Tierney, B. P.; Nakabayashi, N.; Anderson, J. M. *J. Biomed. Mater. Res.* **1991**, *25*, 1397.
19. Ishihara, K.; Nomura, H.; Mihara, T.; Kurita, K.; Iwasaki, Y.; Nakabayashi, N. *J. Biomed. Mater. Res.* **1998**, *39*, 323.
20. Yang, X. P.; Thomas, D. P.; Zhang, X. C.; Culver, B. W.; Alexander, B. M.; Murdoch, W. J.; Rao, M. N. A.; Tulis, D. A.; Ren, J.; Sreejayan, N. *Arterioscler. Thromb. Vasc. Bio.* **2006**, *26*, 85.
21. Thompson, C. J.; Chase, G. G.; Yarin, A. L.; Reneker, D. H. *Polymer* **2007**, *48*, 6913.